

ROMA: ROTary and Movable Antenna

Jiayi Zhang, *Senior Member, IEEE*, Wenhui Yi, Bokai Xu, Zhe Wang, Huahua Xiao, Bo Ai, *Fellow, IEEE*

Abstract—The rotary and movable antenna (ROMA) architecture represents a next-generation multi-antenna technology that enables flexible adjustment of antenna position and array rotation angles of the transceiver. In this letter, we propose a ROMA-aided multi-user MIMO communication system to fully enhance the efficiency and reliability of system transmissions. By deploying ROMA panels at both the transmitter and receiver sides, and jointly optimizing the three-dimensional (3D) rotation angles of each ROMA panel and the relative positions of antenna elements based on the spatial distribution of users and channel state information (CSI), we can achieve the objective of maximizing the average spectral efficiency (SE). Subsequently, we conduct a detailed analysis of the average SE performance of the system under the consideration of maximum ratio (MR) precoding. Due to the non-convexity of the optimization problem in the ROMA multi-user MIMO system, we propose an efficient solution based on an alternating optimization (AO) algorithm. Finally, simulation results demonstrate that the AO-based ROMA architecture can significantly improve the average SE. Furthermore, the performance improvement becomes more pronounced as the size of the movable region and the transmission power increase.

Index Terms—Rotary and movable antennas, multi-user MIMO, spectral efficiency, alternating optimization.

I. INTRODUCTION

As wireless communication evolves, substantial advancements have been made across various dimensions of technology to achieve greater transmission rates and enhanced reliability. Due to the scarcity of spectrum resources, extensive research efforts have been devoted to improving spectral efficiency in wireless communications. In this context, multiple-input multiple-output (MIMO) technology has played a pivotal role, significantly enhancing transmission rates and reliability by harnessing spatial multiplexing and diversity gains [1]. However, traditional MIMO systems are inherently constrained by the fixed position deployment of antenna elements, which limits their full utilization of spatial degrees of freedom. To address the fundamental limitations associated with fixed-position antennas (FPAs), flexible-position antenna systems have recently garnered significant attention as a promising avenue for enhancing MIMO communication performance.

There are notable developments in the flexible-position antenna technology, including fluid antenna (FA) systems, movable antenna (MA) systems, and six-dimensional movable antenna (6DMA) systems. The FA system can dynamically switch a single antenna's position within a small spatial region, exhibiting dynamic properties in terms of possible shapes and locations [2]. The system also comprises multiple fixed positions uniformly distributed within the space, enabling FPAs to switch consistently to the port with the strongest signal. MA systems connect movable antennas to the RF

chain via flexible cables, allowing the antenna positions to be dynamically adjusted by a controller in real time [3]. Compared with traditional MIMO systems with FPAs, this system enables the flexible repositioning of transmit/receive MAs, thereby reshaping the MIMO channel matrix to achieve higher capacity [4]. In the 6DMA system, distributed antennas/arrays can independently move and rotate in a given three-dimensional (3D) space, and collaboratively adjust their steering vectors to achieve favorable channel conditions [5]. Based on the recent studies, we further propose the rotary and movable antennas (ROMA) technique, which can flexibly adjust the positions of antenna elements and array rotation angles of the transceiver to enhance the spatial freedom and channel capacity of the MIMO system without increasing the number of antennas. Compared to FA and MA technologies, ROMA technology enhances spatial coverage by introducing the rotation of antenna planes in 3D space in addition to movable antenna units. In contrast to 6DMA technology, ROMA achieves full coverage by adjusting the deployment parameters of fewer antenna planes in geometric space.

Specifically, this letter studies a ROMA-aided multi-user MIMO system in the downlink transmission. First, we consider a system where both the BS and multiple users are equipped with uniform planar arrays (UPAs) of multiple antennas. Each antenna array can be rotated in 3D space around a fixed axis at the center of the panel, while the antenna elements on the panel can also be repositioned. We then conduct a detailed analysis of the spectral efficiency of the system, and alternately optimize the rotation angles of the BS and user arrays, as well as the relative positions of the antenna elements based on the concept of alternating optimization (AO). This is compared with the heuristic differential evolution (DE) algorithm used in our previous study [6]. Finally, simulation results show that, given the same total number of antennas, the proposed ROMA multi-user MIMO system offers a significant performance gain in average spectral efficiency over traditional FPA system, MA, rotary antenna (RO), and antenna selection (AS).

II. SYSTEM MODEL

We consider downlink communication between a BS and a group of U users that both are equipped with ROMA-aided MIMO systems, as shown in Fig. 1. Denoting $u \in \{1, 2, \dots, U\}$, the system on the BS side and u -th user side is assumed to be uniform planar arrays (UPA) with $M = M_H \times M_V$ antennas and $N^u = N_H^u \times N_V^u$, respectively. M_H and M_V denote the number of transmitting antennas in the horizontal and vertical directions, respectively. Similarly, N_H^u and N_V^u denote the number of antennas equipped on u -th user in the horizontal and vertical directions, respectively. For a UPA-based ROMA-aided MIMO system with P antennas in the horizontal direction and Q antennas in the vertical

J. Zhang, W. Yi, Z. Wang, and B. Ai are with the School of Electronics and Information Engineering, Beijing Jiaotong University, Beijing 100044, P. R. China. H. Xiao is ZTE Corporation, Shenzhen, P. R. China.

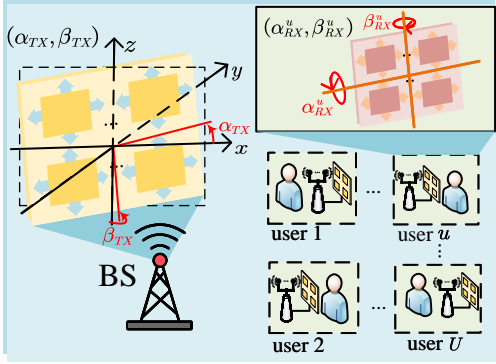


Fig. 1. ROMA-aided multi-user MIMO communication system. direction, the t -th ($t \in \{1, \dots, P \times Q\}$) antenna relative position on the plane can be expressed as

$$\begin{cases} \Delta_{xt}^j = X \cos \alpha - Z \sin \beta \sin \alpha \\ \Delta_{yt}^j = X \cos \alpha + Z \sin \beta \cos \alpha \\ \Delta_{zt}^j = Z \cos \beta, \end{cases} \quad (1)$$

where $j \in \{TX, RX\}$ expresses whether the antenna is located at the transmitter or the receiver, $(X, 0, Z)$ represents the relative coordinates of the t -th antenna element with respect to the center of the ROMA panel. When antenna elements are uniformly distributed on the ROMA panel, $X = (p - \frac{P-1}{2}) d_h$ and $Z = (q - \frac{Q-1}{2}) d_v$, where d_h and d_v are the antenna spacing across the horizontal and vertical direction between adjacent antennas, respectively, α is the rotation angle on the x axis, β is the rotation angle tilt relative to the z axis, and $p = \text{mod}(t-1, P)$ and $q = \lfloor (t-1)/P \rfloor$ are the horizontal and vertical indices of element t , respectively.

By defining the center of the BS plane as the origin of the three-dimensional coordinate system, the position of the m -th ($m = \{1, \dots, M\}$) antenna at the BS can be expressed as $[\Delta_{xm}^{TX}, \Delta_{ym}^{TX}, \Delta_{zm}^{TX}]^T = [r_{tm,x}, r_{tm,y}, r_{tm,z}]^T$, and $\mathbf{r}_{tm} \in \mathbb{R}^3$ is the relative coordinates of the antenna with respect to the center of the transmit panel. In addition, α_{TX} and β_{TX} are the rotation angle of the ROMA planes at the BS end around the x -axis and the tilt relative to the z -axis, respectively. Similarly, the u -th user is equipped with ROMA planes with x -axis rotation angle α_{RX}^u , z -axis rotation angle β_{RX}^u , the horizontal antenna spacing $d_{r,h}^u$, and the vertical antenna spacing $d_{r,v}^u$. We assume that the center of u -th user is located at $[x_u, y_u, z_u]^T$, the n_u -th ($n_u \in \{1, \dots, N_u\}$) antenna at the u -th user can be expressed as $[x_u + \Delta_{xn_u}^{RX}, y_u + \Delta_{yn_u}^{RX}, z_u + \Delta_{zn_u}^{RX}]^T = [r_{rn,x}^u, r_{rn,y}^u, r_{rn,z}^u]^T$, and $\mathbf{r}_{r,n_u} \in \mathbb{R}^3$ is the relative coordinates of the antenna with respect to the center of the user's panel.

In the downlink communication system, the received signal $\mathbf{y}_u \in \mathbb{C}^{N_u}$ at the u -th user can be expressed by

$$\mathbf{y}_u = \sum_{j=1}^U \mathbf{H}_u^* \mathbf{W}_j \mathbf{x}_j + \mathbf{n}_u, \quad (2)$$

where $\mathbf{H}_u \in \mathbb{C}^{M \times N_u}$ is the u -th user's channel, $\mathbf{W}_j \in \mathbb{C}^{M \times N_j}$ ($j \in \{1, 2, \dots, U\}$) is the precoding matrix of the i -th user, $\mathbf{x}_j \in \mathbb{C}^{N_j}$ is the transmitted signal for j -th user with $\mathbb{E}\{|\mathbf{x}_j|^2\} = 1$, $\mathbf{n}_u \in \mathbb{C}^{N_u}$ represents the additive noise vector with independent elements drawn from the complex normal distribution $\mathcal{N}_{\mathbb{C}}(0, \sigma^2)$, where σ^2 denotes the noise power.

The significance of ROMA-aided MIMO system relies on the spatial channel model, by assuming L paths for user channels, the channel is given by [7]

$$\mathbf{H}_u = \sqrt{\frac{1}{L}} \sum_{l=1}^L \beta_{u,l} \mathbf{a}_s(\theta_{u,l}^s, \phi_{u,l}^s) \mathbf{a}_r^T(\theta_{u,l}^r, \phi_{u,l}^r), \quad (3)$$

where L is the number of spatial channel paths, $\beta_{u,l}$ is the complex path gain of the l -th path of u -user's channel, $\mathbf{a}_s(\theta_{u,l}^s, \phi_{u,l}^s) \in \mathbb{C}^M$ and $\mathbf{a}_r(\theta_{u,l}^r, \phi_{u,l}^r) \in \mathbb{C}^{N_u}$ represent the transmit vector and receive vector, respectively. With $\theta_{u,l}^s$, $\phi_{u,l}^s$, $\theta_{u,l}^r$, and $\phi_{u,l}^r$ are transmit azimuth angle, transmit elevation angle, receive azimuth angle, and receive elevation angle, respectively, the m -th element of $\mathbf{a}_s(\theta_{u,l}^s, \phi_{u,l}^s)$ is $[\mathbf{a}_s(\theta_{u,l}^s, \phi_{u,l}^s)]_m = e^{j\boldsymbol{\kappa} \mathbf{r}_{t,m}}$, with $\boldsymbol{\kappa}(\theta_{u,l}^s, \phi_{u,l}^s) = \frac{2\pi}{\lambda} [\cos(\theta_{u,l}^s) \cos(\phi_{u,l}^s), \cos(\theta_{u,l}^s) \sin(\phi_{u,l}^s), \sin(\theta_{u,l}^s)]$ being the transmit wave vector. The n_u -th element of $\mathbf{a}_r(\theta_{u,l}^r, \phi_{u,l}^r)$ is $[\mathbf{a}_r(\theta_{u,l}^r, \phi_{u,l}^r)]_{n_u} = e^{-j\mathbf{k} \mathbf{r}_{r,n_u}}$, with $\mathbf{k}(\theta_{u,l}^r, \phi_{u,l}^r) = \frac{2\pi}{\lambda} [\cos(\theta_{u,l}^r) \cos(\phi_{u,l}^r), \cos(\theta_{u,l}^r) \sin(\phi_{u,l}^r), \sin(\theta_{u,l}^r)]$ being receive wave vector.

III. PERFORMANCE ANALYSIS

Based on (3), the received signal of u -th receiver can be also expressed as

$$\mathbf{y}_u = \mathbf{H}_u^* \mathbf{W}_u \mathbf{x}_u + \sum_{j \neq u}^U \mathbf{H}_u^* \mathbf{W}_j \mathbf{x}_j + \mathbf{n}_u. \quad (4)$$

By denoting $\mathbf{B}_j = \mathbf{H}_u \mathbf{W}_j \in \mathbb{C}^{N_u \times N_j}$, we can obtain the interference matrix $\Xi = \sum_{j=1}^U \mathbf{B}_j \mathbf{B}_j^* - \mathbf{B}_u \mathbf{B}_u^* + \sigma^2 \mathbf{I}_{N_u}$ and the expression for u -user's spectral efficiency (SE) shown as [8]

$$SE_u = \mathbb{E} \left\{ \log_2 \left| \mathbf{I}_N + \mathbf{B}_u \mathbf{H} \Xi^{-1} \mathbf{B}_u \right| \right\}. \quad (5)$$

Based on (3), the (m, n_u) -th element of \mathbf{H}_u can be expressed as [9]

$$\begin{aligned} [\mathbf{H}_u]_{mn_u} &= \sum_{l=1}^L \frac{\beta_{u,l}}{\sqrt{L}} \exp \left[j\boldsymbol{\kappa}(\theta_{u,l}^s, \phi_{u,l}^s) \cdot [r_{tm,x}, r_{tm,y}, r_{tm,z}]^T \right] \\ &\times \exp \left[-j\mathbf{k}(\theta_{u,l}^r, \phi_{u,l}^r) \cdot [r_{rn,x}, r_{rn,y}, r_{rn,z}]^T \right] \\ &= \sum_{l=1}^L \frac{\beta_{u,l}}{\sqrt{L}} h_{mn_u}(l) \stackrel{a}{\approx} \|\mathbf{b}_{um n_u}\|_1 e^{j\pi v_u}, \end{aligned} \quad (6)$$

where the approximate a can be satisfied when the all angles of spatial channel paths hold the linearly independent angle (LIA) condition and arbitrarily large region (ALR) assumption.

Theorem 1. When maximum ratio (MR) precoding is applied, the upper bound of SE_u shown in (5) can be expressed as:

$$SE_u \leq \log_2 \left\{ 1 + \mathbb{E} \left\{ \frac{G_u p_u}{N \sigma^2 + I_{uj}} \right\} \right\} \quad (7)$$

$$\leq \log_2 \left\{ 1 + \frac{G_u p_u}{N \sigma^2} \right\}, \quad (8)$$

where p_u is the transmit power to the u -th user, the channel gain $\|\mathbf{H}_u\|_F^2 \leq \sum_{m=1}^M \sum_{n_u=1}^{N_u} \|\mathbf{b}_{um n_u}\|_1^2 = G_u$, and the Inter-user interference signal $I_{uj} = \sum_{j \neq u}^U \frac{p_j}{G_j} \left(\sum_{n_u=1}^N \sum_{n_j=1}^N \left| \sum_{m=1}^M \sum_{l_1=1}^L \sum_{l_2=1}^L \frac{\beta_{u,l_1}^* \beta_{j,l_2}}{L} h_{mn_u}^*(l_1) h_{mn_j}(l_2) \right|^2 \right)$.

Proof: The proof is provided in Appendix A. \blacksquare

$$SE_u \leq \log_2 \left\{ 1 + \frac{G_u p_u}{N \sigma^2 + \sum_{j \neq u}^U \frac{p_j}{G_j} N^2 (\beta_u^* \beta_j)^2 \frac{\sin^2\left(\frac{\pi}{\lambda}(M_H-1)(\sigma_{s,j}-\sigma_{s,u})\right)}{\sin^2\left(\frac{\pi}{\lambda}(\sigma_{s,j}-\sigma_{s,u})\right)} \frac{\sin^2\left(\frac{\pi}{\lambda}(M_V-1)(\varsigma_{s,j}-\varsigma_{s,u})\right)}{\sin^2\left(\frac{\pi}{\lambda}(\varsigma_{s,u}-\varsigma_{s,j})\right)}} \right\} \quad (9)$$

Corollary 1. *Considering only the Line-of-Sight (LOS) path propagation and assuming that the antenna elements are uniformly distributed on the ROMA panels with the transmit antenna spacing d_{sv} and d_{sh} in the vertical and horizontal direction, respectively, we can further derive the upper bound expression for the SE_u as (9), where $\sigma_{s,i} = d_{sh} \cos \alpha_{TX} \gamma_{s,i} + d_{sh} \sin \alpha_{TX} \eta_{s,i}$ and $\varsigma_{s,i} = d_{sv} \cos \beta \vartheta_{s,i} + d_{sv} \sin \beta_{TX} \cos \alpha_{TX} \eta_{s,i} - d_{sv} \sin \beta_{TX} \sin \alpha_{TX} \gamma_{s,i}$ with $\gamma_{s,i} = \cos(\theta_i^s) \cos(\phi_i^s)$, $\eta_{s,i} = \cos(\theta_i^s) \sin(\phi_i^s)$, $\vartheta_{s,i} = \sin(\theta_i^s)$, and $i \in \{u, j\}$.*

Proof: The proof is provided in Appendix A. ■

Without changing the precoding scheme, the geometric parameters of the ROMA panels can be optimized to continuously reduce the channel correlation among different users, thereby mitigating inter-user interference and enhancing SE performance. However, due to the large number of parameters that need to be optimized in a ROMA multi-user MIMO system, the complexity of joint optimization is excessively high. Therefore, we adopt an alternating optimization (AO) approach to determine suitable geometric configuration parameters.

IV. PROPOSED ALGORITHM

Assuming that all users are equipped with ROMA panels of the same movable region size and number of antennas, we aim to maximize the approximate SE of the ROMA-aided communication network by jointly optimizing the rotation angles of ROMA planes and the coordinates of the antenna units relative to the center of the ROMA plane. The optimization problem is formulated as

$$\text{P1: } \max_{\alpha, \beta, \mathbf{R}_t, \mathbf{R}_r, \mathbf{W}} f(\alpha, \beta, \mathbf{R}_t, \mathbf{R}_r, \mathbf{W}) = \sum_{u=1}^U SE_u / U \quad (10)$$

$$\text{s.t. } \alpha_{TX}, \alpha_{RX}^u \in \{0, \pi\}, \beta_{TX}, \beta_{RX}^u \in \{0, \pi\}, \quad (11)$$

$$\|\mathbf{r}_{tm_p} - \mathbf{r}_{tm_q}\|_2 \geq D, m_p, m_q \in 1, 2, \dots, M, m_p \neq m_q, \quad (12)$$

$$\|\mathbf{r}_{rn_p} - \mathbf{r}_{rn_q}\|_2 \geq D, n_p, n_q \in 1, 2, \dots, N, n_p \neq n_q, \quad (13)$$

$$\sum_{j=1}^U \|\mathbf{W}_j\|_F^2 \leq P_{\max}, \mathbf{r}_{tm} \in \mathcal{O}, \mathbf{r}_{rn_u} \in \mathcal{P}, \quad (14)$$

where $\alpha \in \mathbb{R}^{U+1}$ collects the α_{TX} and α_{RX}^u , $\beta \in \mathbb{R}^{U+1}$ collects the β_{TX} and β_{RX}^u , $\mathbf{R}_t \in \mathbb{R}^{M \times 3}$ collects the coordinates of the BS antenna units relative to the center of the transmission plane $\{\mathbf{r}_{tm}\}_{m=1}^M$, $\mathbf{R}_r \in \mathbb{R}^{U N_u \times 3}$ collects the coordinates of the user antenna units relative to the center of the reception plane $\{\mathbf{r}_{rn_u}\}_{n_u=1}^{N_u}$, \mathcal{O} and \mathcal{P} represent the given region for transmitting and receiving ROMA planes, respectively, D denotes the minimum distance between each pair of antennas, and P_{\max} is the maximum of the BS's transmit power. The problem P1 is non-convex, and it can be solved by optimizing each variable using an AO algorithm.

(1) *Subproblem with respect to \mathbf{W}_j :* The precoding optimization is a non-convex problem, which can be specialized

into a convex problem using algorithms such as fractional programming (FP) [14] or weighted minimum mean square error (WMMSE) [15], followed by gradient descent to solve it. However, in multi-user MIMO scenarios, the above approach requires complex iterations. Therefore, we adopt a closed-form expression for the precoding matrix, e.g., the Zero-Forcing (ZF) method with $\mathbf{W}_u = (\sum_{j=1}^U \mathbf{H}_j \mathbf{H}_j^*)^{-1} \mathbf{H}_u$.

(2) *Subproblem with respect to \mathbf{R}_t :* To separate the non-convex constraint (12), we employ variable splitting by introducing $\{\mathbf{z}_m = \mathbf{r}_{tm}\}_{m=1}^M$. Then, by adding a penalty term to the objective function, the optimization problem with respect to \mathbf{R}_t can be reformulated as

$$\text{P1-a: } \min_{\mathbf{R}_t} -f(\alpha, \beta, \mathbf{R}_t, \mathbf{R}_r, \mathbf{W}) + \rho \sum_{m=1}^M \|\mathbf{r}_{tm} - \mathbf{z}_m\|_2^2, \quad (15)$$

$$\text{s.t. } \sum_{j=1}^U \|\mathbf{W}_j\|_F^2 \leq P_{\max}, \mathbf{r}_{tm} \in \mathcal{O}, \quad (16)$$

where ρ is a penalty factor, initialized with a small positive value $\rho > 0$, and then gradually increased, so that the penalty term approaches zero. In the rectangular region \mathcal{O} , the gradient descent algorithm can be used to obtain at least one solution to the P1-a problem, which is a local optimal solution. Specifically, we utilize PyTorch's automatic differentiation mechanism to perform the iterative computation.

According to the geometry optimal solution proposed in [10], we optimize \mathbf{z}_m appear in the penalty term without any convex approximation by

$$\text{P1-b: } \min_{\{\mathbf{z}_m\}_{m=1}^M} \rho \sum_{m=1}^M \|\mathbf{r}_{tm} - \mathbf{z}_m\|_2^2, \quad (17)$$

$$\text{s.t. } \|\mathbf{z}_m - \mathbf{z}_l\|_2 \geq D, m, l \in 1, 2, \dots, M, m \neq l. \quad (18)$$

To solve the P1-b, We assume that C_l is a circle with center \mathbf{z}_l and radius D . The intersection points between C_l and other circles C_m , as well as the intersection points between C_l and the line passing through \mathbf{z}_l and \mathbf{z}_m , all satisfy constraint (18). Based on the gradient descent algorithm, one of these intersection points is selected to satisfy $\arg \min_{\mathbf{z}_m} \|\mathbf{r}_{tm} - \mathbf{z}_m\|_2^2$, and this intersection point is the optimal \mathbf{z}_m .

(3) *Subproblem with respect to \mathbf{R}_r , α and β :* $\mathbf{R}_r^u \in \mathbb{R}^{N_u \times 3}$ is the u -th user antenna elements relative coordinates in \mathbf{R}_r , and the optimization problems are given by

$$\text{P1-c: } \min_{\{\mathbf{R}_r^u\}_{u=1}^U} -f(\alpha, \beta, \mathbf{R}_t, \mathbf{R}_r, \mathbf{W}) + \rho \sum_{m=1}^M \|\mathbf{r}_{rn_u} - \mathbf{z}_{Ru}\|_2^2, \quad (19)$$

$$\text{s.t. } \sum_{j=1}^U \|\mathbf{W}_j\|_F^2 \leq P_{\max}, \mathbf{r}_{rn_u} \in \mathcal{P}. \quad (20)$$

$$\text{P1-d: } -\min_{\alpha} f(\alpha, \beta, \mathbf{R}_t, \mathbf{R}_r, \mathbf{W}) + \rho \|\alpha - \mathbf{z}_\alpha\|_2^2 \quad (21)$$

$$\text{s.t. } \alpha_{TX}, \alpha_{RX}^u \in \{0, \pi\}, \quad (22)$$

$$\text{P1-e: } -\min_{\beta} f(\alpha, \beta, \mathbf{R}_t, \mathbf{R}_r, \mathbf{W}) + \rho \|\beta - \mathbf{z}_\beta\|_2^2 \quad (23)$$

$$\text{s.t. } \beta_{TX}, \beta_{RX}^u \in \{0, \pi\}. \quad (24)$$

Similar to the subproblem with respect to \mathbf{R}_t , we employ variable splitting by introducing $\{\mathbf{z}_{Ru} = \mathbf{r}_{rn_u}\}_{n_u=1}^N$, $\mathbf{z}_\alpha = \alpha$

and $\mathbf{z}_\beta = \beta$. Based on the solution approaches for P1-a and P1-b, the objectives in P1-c, P1-d, and P1-e are alternately optimized. Through multiple iterations, at least one set of optimal solutions can be obtained.

Algorithm 1 The AO Algorithm for ROMA-aided multi-user MIMO system

- 1: Initialize the optimization variables, compute the average SE SE_e based on the initial variables, initial average SE $SE_0 = -1$.
 - 2: **while** $SE_e - SE_0 > 10^{-5}$ **do**
 - 3: Update \mathbf{R}_t by P1-a, and update \mathbf{z}_{Rt} by P1-b.
 - 4: **for** $u = 1, 2, \dots, U$ **do**
 - 5: Update \mathbf{R}_r^u by P1-c, and update \mathbf{z}_{Ru} by P1-b.
 - 6: **end for**
 - 7: Update α by P1-d, update \mathbf{z}_α by P1-b.
 - 8: Update β by P1-e, update \mathbf{z}_β by P1-b.
 - 9: $SE_0 = SE_e$, and update the SE_e based on the updated parameters.
 - 10: **end while**
-

V. SIMULATION RESULTS AND DISCUSSIONS

In this section, we evaluate the proposed ROMA-aided multi-user MIMO system based on the achievable average SE. Unless otherwise specified, the simulation parameters are set as follows. We configure that the number of users $U = 4$, the antenna numbers of the BS $M = M_H \times M_V = 3 \times 3$, and the number of antennas at the users is configured to be identical to that at the BS. Besides, we set the carrier frequency $f_c = 2.1\text{GHz}$, the speed of the light c , the wavelength $\lambda = c/f_c$. The transmit power of the BS for each user is p . Moreover, the user positions are randomly distributed within a region centered around the BS panel.

For comparison, we provide the following baselines:

- MA [3]: The transceiver panels are non-rotatable, while the antenna elements can be repositioned on the antenna panels based on the joint optimization.
- RO [12]: The relative positions of the antenna elements on the panel are fixed with the antenna spacing of $\lambda/2$, while the entire panel can rotate around its center axis.
- AS [13]: The transceivers are equipped with 12 antennas, arranged in a fixed square array with an antenna spacing of $\lambda/2$. The ports are fixed, and the antenna arrays cannot be rotated. The algorithm jointly optimizes the selection of 9 antennas to operate on each side.

In Fig. 2, we compare the relationship between number of iterations and average SE by varying transmit power p and optimization algorithm with $A = 2.5\lambda$. Compared to the heuristic DE algorithm [6], the AO algorithm employed in the ROMA architecture proposed in this letter converges more quickly. Moreover, during the finite number of iterations in this simulation, the AO algorithm achieves a higher average SE performance compared to the DE algorithm. It can also be observed that as the transmit power p increases, the ROMA architecture reaches a higher convergence value by optimizing the antenna geometric parameters.

In Fig. 3, we demonstrate the average SE versus the normalized region size A for the ROMA-aided MIMO system

and the baselines. It can be observed that the average SE of the ROMA-aided MIMO systems significantly outperforms other system architectures. Furthermore, the systems assisted by ROMA and MA show an increase in SE as the normalized region size A expands, while other architectures remain relatively stable. This is because the RO, AS and FPA architectures fix the positions of the antenna elements, so the expansion of the region size does not affect system performance. However, the performance improvement brought by rotating the antenna panels is evident. In summary, the ROMA-aided MIMO system exhibits a significant performance enhancement, which further improves as the movable region size increases.

Fig. 4 shows the average SE versus the transmit power p for the ROMA-aided MIMO systems and the baselines with $A = 2.5\lambda$. It can be observed that as the transmission power p increases, the average SE of the ROMA- and MA-aided MIMO systems improves, and the ROMA-aided system demonstrating superior performance compared to the MA-aided system. Moreover, the average SE of the MIMO systems assisted by the RO, AS, and FPA architectures remains relatively stable with p . This is because that without altering power distribution and precoding, an increase in transmission power simultaneously enhances both the desired signal power and the interference signal power. However, significant performance improvements are achieved through the movement of antenna element positions on the antenna panel.

VI. CONCLUSION

In this letter, we consider a new ROMA-aided multi-user MIMO system, where both the transmitter and receivers are equipped with antenna arrays based on the ROMA planes. These planes are capable of 3D rotation around their center, while the antenna elements on the array can be moved within the plane based on the spatial distribution of users and varying transmission power. Additionally, we propose an AO algorithm to jointly optimize the antenna geometric parameters, including the panel rotation angles and the relative positions of the antenna elements, at both the BS and the user side to maximize the average SE. Numerical results demonstrate that the AO algorithm employed in the proposed system outperforms the heuristic DE algorithm. Furthermore, compared to MIMO systems assisted by MA, RO, AS, and FPA, the proposed system achieves superior performance, with more significant performance improvements observed as the movable region size increases and transmission power is enhanced.

APPENDIX A

PROOF OF THEOREM 1 AND COROLLARY 1

Considering the MR precoding, the normalized precoding matrix \mathbf{W}_u is given by $\mathbf{W}_u = p_u \mathbf{H}_u / \|\mathbf{H}_u\|_F$. Based on the analysis of SE in [11], we can reformulate the SE_u with high signal-to-noise ratio (SNR) in (5) as

$$\begin{aligned}
 SE_u &= \mathbb{E}\left\{\log_2\left\{1 + \frac{\frac{p_u}{\|\mathbf{H}_u\|_F^2} \|\mathbf{H}_u^* \mathbf{H}_u\|_F^2}{N\sigma^2 + \sum_{j \neq u}^U \frac{p_j}{\|\mathbf{H}_j\|_F^2} \|\mathbf{H}_u^* \mathbf{H}_j\|_F^2}\right\}\right\} \\
 &\leq \mathbb{E}\left\{\log_2\left\{1 + \frac{\|\mathbf{H}_u^*\|_F^2 p_u}{N\sigma^2 + \sum_{j \neq u}^U \frac{p_j}{\|\mathbf{H}_j\|_F^2} \|\mathbf{H}_u^* \mathbf{H}_j\|_F^2}\right\}\right\}.
 \end{aligned} \tag{25}$$

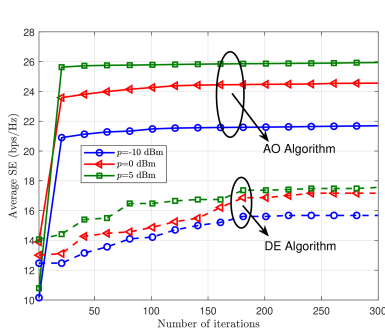


Fig. 2. Average SE versus the number of iterations for different optimization algorithms with different size A for different system architectures with $p = 30$ dBm. The parameters of the channel model are the same as those in [7] with $L = 15$.

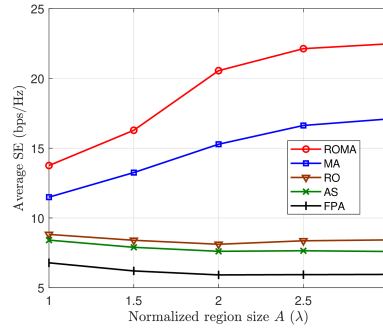


Fig. 3. Average SE versus the normalized region size A for different system architectures with $p = 30$ dBm. The parameters of the channel model are the same as those in [7] with $L = 15$.

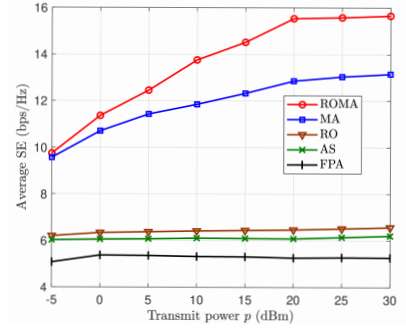


Fig. 4. Average SE versus the transmit power p for different system architectures with $A = 2.5\lambda$.

According to [9, Theorem 1], under the LIA condition and the ALR assumption, there always satisfy

$$\left| \sum_{l=1}^L \frac{\beta_{u,l}}{\sqrt{L}} h_{mn_u}(l) - \|\mathbf{b}_{umn_u}\|_1 e^{j\pi v_u} \right| \leq \delta, \quad (26)$$

with any small positive number $\delta \ll 1$. Therefore, by denoting $\sum_{m=1}^M \sum_{n_u=1}^{N_u} \|\mathbf{b}_{umn_u}\|_1^2 = G_u$, we can substitute the channel matrix and the normalized precoding matrix to proof (7) in Theorem 1. Under ideal conditions, the antenna element positions and rotation angles of the ROMA panels are the optimal states, ensuring that the propagation channels of different users are mutually orthogonal. This leads to the optimal SE_u , as shown in (8).

Assuming only the LOS path propagation and antenna elements are uniformly distributed on the ROMA panels, we can obtain that

$$\mathbf{R}(n_u, n_j) = \sum_{m=1}^M h_{mn_u}^* h_{mn_j} \quad (27)$$

$$= \sum_{m_2=1}^{M_V} \sum_{m_1=1}^{M_H} \exp[-j \frac{2\pi}{\lambda} (r_{tm,x}\gamma_{s,u} + r_{tm,y}\eta_{s,u} + r_{tm,z}\vartheta_{s,u})] \times \exp[j \frac{2\pi}{\lambda} (r_{tm,x}\gamma_{s,j} + r_{tm,y}\eta_{s,j} + r_{tm,z}\vartheta_{s,j})] \mathcal{E}_u \mathcal{Z}_j, \quad (28)$$

where $\mathcal{E}_u = \exp[j \frac{2\pi}{\lambda} (r_{rn_u,x,u}\gamma_{r,u} + r_{rn_u,y,u}\eta_{r,u} + r_{rn_u,z,u}\vartheta_{r,u})]$, and $\mathcal{Z}_j = (\mathcal{E}_j)^*$. Then, we simplify the phase in (28) with

$$r_{tm,x}\gamma_{s,i} + r_{tm,y}\eta_{s,i} + r_{tm,z}\vartheta_{s,i} = m_1 \sigma_{s,i} + m_2 \varsigma_{s,i} - \frac{M_H - 1}{2} \sigma_{s,i} - \frac{M_V - 1}{2} \varsigma_{s,i}, \quad (29)$$

where $i \in \{u, j\}$, m_1 and m_2 are the horizontal and vertical indices of m -th element, respectively. Therefore, the expression SE_u can be given by

$$\begin{aligned} \mathbf{R}(n_u, n_j) &= \sum_{m=1}^M h_{mn_u}^* h_{mn_j} \\ &= \sum_{m_2=0}^{M_V-1} \sum_{m_1=0}^{M_H-1} \exp[j \frac{2\pi}{\lambda} (m_1 (\sigma_{s,j} - \sigma_{s,u}) + m_2 (\varsigma_{s,j} - \varsigma_{s,u})) \\ &\quad - \frac{M_H - 1}{2} (\sigma_{s,j} - \sigma_{s,u}) - \frac{M_V - 1}{2} (\varsigma_{s,j} - \varsigma_{s,u})] \mathcal{E}_u \mathcal{Z}_j \\ &\stackrel{b}{=} \frac{\exp[-j \frac{\pi(M_H-1)}{\lambda} (\sigma_{s,j} - \sigma_{s,u})] - \exp[j \frac{\pi(M_H-1)}{\lambda} (\sigma_{s,j} - \sigma_{s,u})]}{1 - \exp[j \frac{2\pi}{\lambda} (\sigma_{s,j} - \sigma_{s,u})]} \\ &\quad \times \frac{\exp[-j \frac{\pi(M_V-1)}{\lambda} (\varsigma_{s,j} - \varsigma_{s,u})] - \exp[j \frac{\pi(M_V-1)}{\lambda} (\varsigma_{s,j} - \varsigma_{s,u})]}{1 - \exp[j \frac{2\pi}{\lambda} (\varsigma_{s,j} - \varsigma_{s,u})]} \mathcal{E}_u \mathcal{Z}_j \\ &\stackrel{c}{\approx} \mathcal{E}_u \mathcal{Z}_j \frac{\sin(\frac{2\pi}{\lambda} \frac{M_H-1}{2} (\sigma_{s,j} - \sigma_{s,u}))}{\sin(\frac{1}{2} \frac{2\pi}{\lambda} (\sigma_{s,j} - \sigma_{s,u}))} \frac{\sin(\frac{2\pi}{\lambda} \frac{M_V-1}{2} (\varsigma_{s,j} - \varsigma_{s,u}))}{\sin(\frac{1}{2} \frac{2\pi}{\lambda} (\varsigma_{s,j} - \varsigma_{s,u}))}, \quad (30) \end{aligned}$$

where the approximate b is the geometric sum formula $\sum_{n=0}^{M-1} x^n = (1 - x^M)/(1 - x)$ and the approximate c is the trigonometric identity $\sin(x) = (e^{jx} - e^{-jx})/(2j)$. Substituting (30) into (7), we can complete the proof of Corollary 1.

REFERENCES

- [1] B. Xu, J. Zhang, H. Du, Z. Wang, Y. Liu, D. Niyato, B. Ai, and K. B. Letaief, "Resource Allocation for Near-Field Communications: Fundamentals, Tools, and Outlooks," *IEEE Wireless Commun.*, vol. 31, no. 5, pp. 42-50, Oct. 2024.
- [2] W. K. New, K.-K. Wong, H. Xu, C. Wang, F. R. Ghadi, J. Zhang, J. Rao, R. Murch, P. Ramirez-Espinosa, D. Morales-Jimenez, C.-B. Chae, and K.-F. Tong, "A tutorial on fluid antenna system for 6G networks: Encompassing communication theory, optimization methods and hardware designs," *IEEE Commun. Surv. Tuts.*, early access, Nov. 2024.
- [3] W. Mei, X. Wei, B. Ning, Z. Chen, and R. Zhang, "Movable-Antenna Position Optimization: A Graph-Based Approach," *IEEE Wireless Commun. Lett.*, vol. 13, no. 7, pp. 1853-1857, Jul. 2024.
- [4] L. Zhu, W. Ma, and R. Zhang, "Movable Antennas for Wireless Communication: Opportunities and Challenges," *IEEE Commun. Mag.*, vol. 62, no. 6, pp. 114-120, Jun. 2024.
- [5] X. Shao, Q. Jiang, and R. Zhang, "6D Movable Antenna Based on User Distribution: Modeling and Optimization," *IEEE Trans. Wireless Commun.*, vol. PP, no. 99, pp. 1-1, Oct. 2024.
- [6] W. Yi, J. Zhang, Z. Wang, H. Xiao, and B. Ai, "Performance analysis of XL-MIMO with rotary and movable antennas for high-speed railway," *arXiv:2412.03940*, 2024.
- [7] E. Björnson and L. Sanguinetti, "Rayleigh fading modeling and channel hardening for reconfigurable intelligent surfaces," *IEEE Wireless Commun. Lett.*, vol. 10, no. 4, pp. 830-834, Apr. 2021.
- [8] Z. Wang, J. Zhang, E. Björnson, D. Niyato, and B. Ai, "Optimal Bilinear Equalizer for Cell-Free Massive MIMO Systems over Correlated Rician Channels," *arXiv:2407.18531*, 2024.
- [9] L. Zhu, W. Ma, Z. Xiao, and R. Zhang, "Performance analysis and optimization for movable antenna aided wideband communications," *arXiv:2401.08974*, 2024.
- [10] Y. Jin, Q. Lin, Y. Li, and Y. C. Wu, "Handling distance constraint in movable antenna aided systems: A general optimization framework," in *Proc. IEEE SPAWC*, pp. 396-400, Sep. 2024.
- [11] M. Franceschetti, M. D. Migliore, and P. Minero, "The capacity of wireless networks: Information-theoretic and physical limits," *IEEE Trans. Inf. Theory*, vol. 55, no. 8, pp. 3413-3424, Aug. 2009.
- [12] J. C. Ruiz-Sicilia, M. Di Renzo, P. Mursia, A. Kaushik, and V. Sciancalepore, "Spatial Multiplexing in Near-Field Line-of-Sight MIMO Communications: Paraxial and Non-Paraxial Deployments," *IEEE Trans. Green Commun. Netw.*, early access, Jun. 2024.
- [13] H. Li, L. Song and M. Debbah, "Energy efficiency of large-scale multiple antenna systems with transmit antenna selection," *IEEE Trans. Commun.*, vol. 62, no. 2, pp. 638-647, Feb. 2014.
- [14] Z. Zhang and L. Dai, "A Joint Precoding Framework for Wideband Reconfigurable Intelligent Surface-Aided Cell-Free Network," *IEEE Trans. Signal Process.*, vol. 69, pp. 4085-4101, Jun. 2021.
- [15] Q. Shi, M. Razaviyayn, Z.-Q. Luo, and C. He, "An Iteratively Weighted MMSE Approach to Distributed Sum-Utility Maximization for a MIMO Interfering Broadcast Channel," *IEEE Trans. Signal Process.*, vol. 59, no. 9, pp. 4331-4340, Apr. 2011.